

A new biometric identity recognition system based on a combination of superior features in finger knuckle print images

Hadis HEIDARI[✉], Abdolah CHALECHALE*[✉]

Department of Computer Engineering, Faculty of Engineering, Razi University, Kermanshah, Iran

Received: 03.06.2019

Accepted/Published Online: 02.09.2019

Final Version: 27.01.2020

Abstract: Biometric methods are among the safest and most secure solutions for identity recognition and verification. One of the biometric features with sufficient uniqueness for identity recognition is the finger knuckle print (FKP). This paper presents a new method of identity recognition and verification based on FKP features, where feature extraction is combined with an entropy-based pattern histogram and a set of statistical texture features. The genetic algorithm (GA) is then used to find the superior features among those extracted. After extracting superior features, a support vector machine-based feedback scheme is used to improve the performance of the biometric system. Two datasets called Poly-U FKP and FKP are used for performance evaluation. The proposed method managed to achieve 94.91% and 98.5% recognition rates on the Poly-U FKP and FKP datasets and outperformed all of the existing methods in this respect. These results demonstrate the potential of this method as a simple yet effective solution for FKP-based identity recognition.

Key words: Entropy-based pattern, texture feature, genetic algorithm, biometric, finger knuckle print

1. Introduction

The main objective of biometric identification systems is to detect and verify the identity of people based on their behavioral and physiological features [1], including weight, voice, gait, fingerprints [2], iris [3–5], retina [6–8], ear shape [9], palm lines [10], facial features [11], and other characteristics. So far, many biometric identification methods have been proposed. Finger knuckle print (FKP)-based recognition methods are reliable authentication approaches, including orientation and magnitude information extracted by Gabor filtering, Markov models, grade schemes, and the other texture descriptors. In the studies carried out by Zhang et al., a Gabor filter-based coding scheme was used for FKP recognition [12]. In [13], the local orientation information extracted by Gabor filters and the Fourier transform coefficients were considered, respectively, as local and global features of FKP images. Woodard et al. used a sensor to create a three-dimensional hand dataset and then utilized the features extracted from fingers for identification [14]. However, the cost, size, and weight of the sensor and the prolonged data retrieval and processing of this method limit its use as a practical biometric solution. In a study by Ferrer et al., they developed a biometric identification system that considers the FKP as a biometric feature and uses the hidden Markov model in the identification phase [15]. However, this method has an extensive processing phase and works well only when a limited amount of data is being processed. Rawikanth et al. used the FKP region to detect the orientation and scale of finger images. However, the subspace analysis method used in the feature extraction phase was not able to extract the features of the knuckles very effectively [16].

*Correspondence: chalechale@razi.ac.ir

In [17], Zhao et al. proposed a new algorithm for extracting edge attributes from knuckle images by use of a grade identification scheme. In this method, knuckle line features are extracted through the binarization of images, but it is difficult to set a proper threshold value for the binarization operation. In the method proposed in [18] for Gabor filter-based feature extraction from FKP images, principal component analysis (PCA) and linear discriminant analysis (LDA) were used to reduce the dimensions of the features. Morales et al. combined the Gabor filter with a scale-invariant feature transform (SIFT) for FKP feature extraction in a method they called OE-SIFT [19]. Nigam et al. also used the Gabor filter to develop a FKP-based identification system [20]. Although this method has good accuracy, the high dimensionality of Gabor features means it has extensive memory consumption. Moreover, the high computational time and complexity of Gabor feature extraction reduce the speed of identification. Ozkaya et al. [21] used a discriminative common vector-based FKP recognition, which was in fact an intraclass scatter matrix, for feature extraction from FKP images. While being desirably accurate, this method had high computational complexity. In [22], knuckle texture variations and the entropy function were used for FKP-based identification. This method involved combining the scores of middle and index fingers of the left and right hands at the fuzzy decision level. In addition, deep learning is a subfield of machine learning, which uses a set of approaches that attempt to model high-level abstractions present in data by using a deep architecture, having linear and nonlinear transformation functions [23]. A deep texture encoding network (DeepTEN) was introduced in [24] by using an encoding layer on top of convolutional layers. In this scheme, a Fisher vector in a convolutional neural network was trained end to end.

Recent studies have shown that knuckles have unique patterns that vary from person to person and can therefore be exploited as a feature in the development of potentially powerful biometric identification systems. Many of the methods proposed so far for this purpose are not sufficiently accurate, and those that are [1,18] have high computational time and complexity, which renders them inapplicable for fast identification. Therefore, there is a need for both faster and more accurate biometric identification systems.

In this study, after creating a dataset of 5450 FKP images, we create a simple but powerful and highly accurate identification method based on FKP features. The proposed method involves extracting the histogram of patterns based on entropy at different levels and effective texture features. While extracting the texture features, the uniformity criterion is used to improve robustness against image rotation. A metaheuristic genetic algorithm (GA) is used to find the superior features among those extracted. After extracting the superior features, a support vector machine (SVM)-based feedback scheme is used to improve the performance of biometric identification. The proposed method allows for more accurate detection of identity based on FKP patterns. The paper will demonstrate the high effectiveness of the method in comparison with existing alternatives.

The remainder of this article is organized as follows: Section 2 describes the feature extraction scheme, including the involved texture patterns and parameters. Section 3 presents the proposed biometric identification procedure including preprocessing, feature extraction, selection of superior features, and classifications. Section 4 demonstrates the validity of the method and compares its results with other methods. Finally, Section 5 concludes the paper and provides a few suggestions for future work.

2. Texture feature extraction

Extraction of visual content from images is one of the key phases of identification systems. Since the features present in a FKP vary from person to person, it can be used for precise identification of individuals, provided that prominent distinctive features of knuckles can be efficiently extracted. For more accurate comparison of

knuckle patterns, only significant features should be encoded rather than all information in the FKP texture. To describe the texture features extracted from the images, it is necessary to first review the local binary pattern (LBP) and the texture features that are used in the proposed identification system.

2.1. Local binary pattern (LBP)

The LBP is an operator for texture analysis. In this operator, each central pixel is compared to its eight neighboring pixels. This operator writes 1 in any neighbor pixel whose value is equal to or greater than the central pixel's value and writes 0 in others. After calculating an eight-bit binary number for each central pixel [25], the histogram of the eight-bit patterns is considered as the texture feature vector, which has 256 bins. Naturally, the rotation of the image will change the patterns.

2.2. Entropy-based patterns

In LBP, since comparisons are made between two pixel values, even small changes have a large impact on the pattern. In the proposed method, processing starts from the pixel located in the fourth row and the fourth column, and it involves a comparison between each central pixel and the 24 pixels positioned around it. Of these 24 neighbors, eight will be positioned at a 3-pixel distance from the center, another eight will be positioned at a 2-pixel distance, and the last eight will be at a 1-pixel distance from the central pixel. The set of pixels selected for a central pixel is shown in Figure 1.

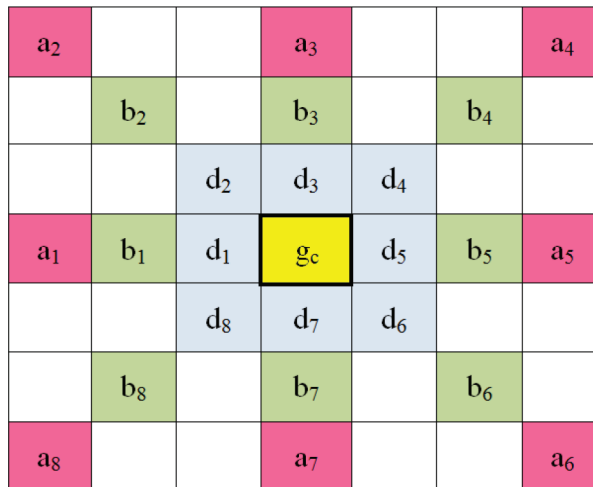


Figure 1. Set of neighbor pixels considered for a central pixel.

In this figure, the value of the central pixel is denoted by g_c , the values of neighbor pixels within the 3-pixel distance of this center are denoted by $a = [a_1, a_2, \dots, a_8]$, the values of neighbor pixels within the 2-pixel distance of this center are denoted by $b = [b_1, b_2, \dots, b_8]$, and the values of neighbor pixels within the 1-pixel distance of this center are denoted by $d = [d_1, d_2, \dots, d_8]$. An array of the values of these neighbor pixels is defined as $ne = [a, b, d]$. An array of the set of neighbor pixels and the central pixel (with $q = 25$ members) is also defined as $nec = [ne, g_c]$. In the proposed scheme, for each central pixel, there is a $u \times v$ pixel neighborhood, according to which a kernel is defined as named K . The values of this kernel represent the significance of the neighbor pixel for the central pixel. The pixels positioned at a 1-pixel distance from a central pixel have the highest significance (and therefore a coefficient of 4) and the pixels other than the 24 selected pixels have the

least significance. In other words, in the images of the knuckle area, pixels positioned around a central pixel contain information with different values for that pixel, which have to be given different weights in the analysis. The set of pixels positioned at a 1-pixel distance from the central pixel typically has a smaller coefficient of variation than the set of those at a 3-pixel distance from the center. Therefore, different multipliers are applied to these neighbors to amplify these differences. The second step is to calculate the weighted average of the set of neighbor pixels using Equation 1.

$$WM = \frac{1}{Y} \sum_{i=1}^u \sum_{j=1}^v (G_{i,j} \times K_{i,j}) \quad (1)$$

Here, Y is the sum of coefficients in the kernel K in the $u \times v$ neighborhood, $G_{i,j}$ is the intensity of the pixel positioned in row i and column j of the subimage being processed, and $K_{i,j}$ is the significance coefficient defined for row i and column j in kernel K. Here, u and v are both 7. Array k includes the set of neighbor pixels with a significance coefficient of 1, and n is the number of pixels adjacent to the central pixel at a specific level while parameters l, z, and e denote the number of levels, the significance coefficients, and the set of pixels considered at the processing level, respectively. The third step is to calculate the following function for the set of neighbor pixels at different levels, where $l = 1,2,3,4$, $z = 4,3,2,1$, and $e = d,b,a,k$.

$$E_{l,z,e} = \frac{z}{n} \sum_{i=1}^n (ze_i \times \ln(ze_i)) \quad (2)$$

These functions, which have been derived from the definition of entropy function [26], serve as a means to extract superior features from images so as to improve the accuracy of the proposed identification system. Next, the value of the central pixel is obtained as follows:

$$TP_N = \sum_{i=1}^N (g_i \times 2^{i-1}) \quad (3)$$

g_i is 0 if $a_i \geq g_c + E_{3,2,a} - WM$, $b_i \geq g_c + E_{2,3,b} - WM$, and $d_i \geq g_c + E_{1,4,d} - WM$; otherwise, g_i is 1. N is the number of pixels at a 1-pixel distance from the central pixel. Using this scheme for the comparison of the central pixel with its neighbors, one can improve the accuracy of identification by running a statistical analysis on FKP images and considering different levels of significance for the sets of pixels at different image levels. The reason for choosing 8-bit patterns at different distances from central pixels is the curved lines that appear in FKP images. These lines contain valuable information that is worthy of consideration. Execution of the described processes at different levels results in the extraction of texture features that play a key role in identification. After extracting the patterns for each pixel (x, y) in the input image of the size $M_x \times M_y$, Equation 4 is used to find a texture pattern by generating a histogram from a bin of 2^N codes.

$$H(\alpha) = \sum_{i=4}^{M_x-4} \sum_{j=4}^{M_y-4} (f(TP_N(i, j), \alpha)) \quad (4)$$

$$f(aa, bb) = \begin{cases} 1 & \text{if } aa=bb \\ 0 & \text{else} \end{cases} \quad (5)$$

The proposed descriptor also takes uniform patterns into account [27]. For this purpose, the uniformity criterion U is defined as the number of successive bit flips (1 to 0 or 0 to 1) in the N -bit texture pattern C .

$$U(TP_N) = |C(N) - C(1)| + \sum_{i=2}^N (|C(i) - C(i-1)|) \quad (6)$$

For example, the strings 00101100 and 11110111 will have U values of 4 and 2, respectively. In the uniform pattern, the number of flips in an N -bit binary string is limited to $U \leq 2$. All nonuniform patterns in the N -bit string have $U \geq 3$. Here, it should be noted this uniformity criterion makes the descriptor robust against image rotation, because changes in the first and eighth bits are considered an important factor. The use of this uniformity criterion for texture patterns at different levels reduces the number of features from $2N$ in the bin to $N+2$.

2.3. Statistically significant features of FKP

In addition to the above patterns, the following statistical features can contribute to the analysis of different images, including FKP images [28].

$$\mu = \frac{1}{q-1} \sum_{i=1}^{q-1} k_i \quad RMS = \sqrt{\frac{1}{q-1} \sum_{i=1}^{q-1} k_i^2} \quad V = \frac{\sum_{i=1}^{q-1} (k_i - \mu)^2}{q-2} \quad Ske = \frac{\sum_{i=1}^{q-1} (k_i - \mu)^3}{(q-1)\sigma^3} \quad (7)$$

$$Ku = \frac{\sum_{i=1}^{q-1} (k_i - \mu)^4}{(q-1)\sigma^4} \quad P = \frac{1}{q-1} \sum_{i=1}^{q-1} k_i^2 \quad pp = \max(k_i) - \min(k_i) \quad CF = \frac{pp}{RMS} \quad (8)$$

Equations (7) and (8) indicate the arithmetic mean, root mean square, variance, skewness, kurtosis, signal power, peak to peak amplitude, and crest factor, respectively. Also, k_i , σ^3 , and σ^4 are pixel values in the fourth level, third moment, and fourth level. These statistical texture features have been shown to be very effective in image analysis. To obtain the second part of the feature vector, we compute the above statistical parameters for every subimage and use the highest obtained value in the feature vector. The highest value of $E_{4,1,k}$ in subblocks is also considered as a significant texture feature. In this step, pixel values, mean, variance, third and fourth moments, an entropy-based function, and the difference between largest and smallest pixel values are considered as significant factors of FKP image analysis.

3. Proposed biometric system based on FKP

This section explains the general procedure of the proposed identification system, the preprocessing steps that are necessary for extracting FKP features, calculation of FKP feature vectors, selection of superior features, and finally FKP-based identification.

3.1. Proposed identification process

The proposed biometric identification system consists of the five main stages illustrated in Figure 2: image acquisition using a wooden device, preprocessing (hand skin detection and FKP extraction), feature extraction using the proposed texture descriptor, extraction of superior features in FKP images using a GA, and

classification using a support vector machine. After receiving the images of the hands of different people, a preprocessing phase is carried out to extract the FKP areas. Next, the texture features of each image in the dataset are extracted and then processed by the GA to form the set of superior features. Finally, the SVM classifier is used for identification based on chosen features.

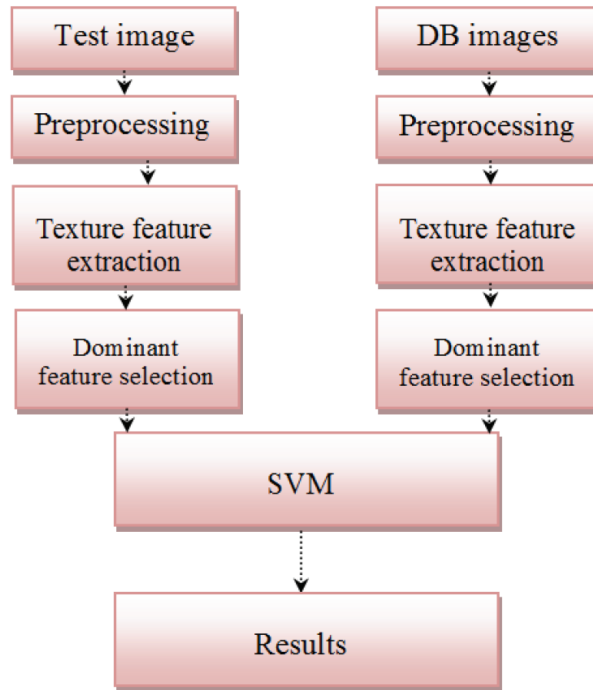


Figure 2. Flowchart of the proposed identification system.

3.2. Preprocessing steps

This section describes the steps followed to obtain FKP images and extract areas of interest. For this purpose, a set of hand images was collected by an imaging setup. The setup included a Canon SX 600 HS digital camera fixed on a frame and a flat wooden board for participants to rest their hands on. Images were taken with the size of 4606×3456 pixels. To isolate the FKP areas, the obtained images must be subjected to a skin extraction procedure. This procedure is carried out in the CMYK color space [29], which consists of cyan (between blue and green), magenta (reddish color), yellow, and black. The images are mapped from the RGB color space to CMYK. Then, after thresholding of the color components and limiting the color components in this space, the skin areas are detected. Having the center of gravity of the hand and the boundary points with the least distance from this center, the radius of the palm area can be computed. The square structures are then used to separate the palm and wrist area from the image. The five fingers are then extracted by subtracting the obtained area from the original image. Figure 3 shows the separation of five fingers from the rest of the image as an example. To separate the FKP area, it is enough to have the center of gravity of each finger, its length, and its orientation. Figure 4 shows the center of gravity (x_c, y_c) , length (L), and orientation (O) of the index finger for an example image. The areas of interest are extracted by calculating these three components (center,

length, and orientation) for each finger. The FKP of the right hand is obtained by the following:

$$x_2 = x_1 - ri(j)[\cos(O) \quad -\cos(O)] \quad y_2 = y_1 - ri(j)[-sin(O) \quad sin(O)] \quad (9)$$

$$x_1 = \min(x_c + \frac{L}{2}[\cos(O) \quad -\cos(O)]) \quad y_1 = \min(y_c + \frac{L}{2}[-sin(O) \quad sin(O)]) \quad (10)$$



Figure 3. Extraction of fingers from a hand image.

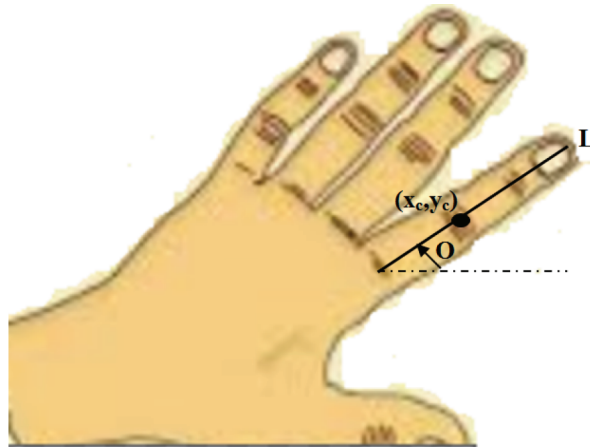


Figure 4. Center (x_c, y_c) , length (L) , and orientation of the index finger under the angle O .

Here, (x_2, y_2) are the coordinates of the upper left corner of the subimage related to the FKP. After finding this point, moving 75 pixels right and 75 pixels down gives the bottom right corner coordinates of the FKP subimage. The reason for choosing 75 pixels is that the FKP area of each hand is approximately 75×75 pixels. Having these two coordinates, the area of interest can be cropped from the image. In this equation, ri is an array with values $ri = [120 \ 200 \ 230 \ 230 \ 180]$ for each finger of the right hand, (x_c, y_c) are the coordinates of the center of gravity of each finger, L is the length of each finger, O is the orientation of each finger, and $j = 1, 2, 3, 4, 5$ is the index of each finger. Similarly, Equation 11 gives the coordinates of the upper left corner of the FKP subimage for the left hand.

$$x_3 = x_1 - le(j)[\cos(O) \quad -\cos(O)] \quad y_3 = y_1 - le(j)[-sin(O) \quad sin(O)] \quad (11)$$

Here, le is an array with values $le = [180 \ 230 \ 230 \ 200 \ 120]$ for each finger of the left hand. Because of the different position of the fingers of the left and right hands, the arrays ri and le are initialized empirically. These two equations are used to separate the FKP areas from the rest of the hand. Note that when photographing,

participants were asked to hold their fingers straight, as it is crucial for the precise extraction of FKP areas. However, in a limited number of images, the FKP areas were not accurately separated and this process had to be done manually. After extracting the areas of interest, the next step is to compute texture patterns and find significant features.

3.3. Extraction of texture features from FKP images

Extraction of texture features is one of the most important steps of pattern recognition. As mentioned, the texture features of the FKP of each person are unique. For accurate identification of individuals, only the significant features of the FKP should be coded to ensure that the comparison between texture patterns remains effective. The proposed method makes use of an entropy-based pattern extraction technique, which it applies to the set of pixels. This technique involves considering a set of pixels positioned around each pixel at different levels and then conducting a series of calculations based on the weighted average and the entropy-based functions to obtain a set of binary patterns. The histogram of these patterns and the set of texture features including the mean, root mean square, variance, skewness, kurtosis, signal power, peak to peak amplitude, crest factor, and entropy function value at the fourth level of images provide a way to extract texture features that are of significant value for identification.

To reach a higher level of accuracy, the third part of the texture feature vector is obtained by considering the histogram of binary patterns, which are given by coding schemes known as gradient ordinal relation pattern (GORP) and star gradient ordinal relation pattern (SGORP), as another feature [20]. In the GORP coding scheme, for each central pixel g_c , the set of neighbor pixels $d[i]$, $i = 1, 2, \dots, N$, is replaced with the set of their gradients $Gra[i]$. Then Equation 12 is used to compute the bits of binary patterns.

$$gorp[i] = \begin{cases} 1 & \text{if } Gra[i] \geq 0 \\ 0 & \text{else} \end{cases} \quad (12)$$

In the SGORP coding scheme [20], however, the values of the patterns are calculated as follows:

$$sgorp[1] = sgorp[2] = \begin{cases} 1 & \text{if } |Gra[1] - Gra[5]| \geq \Gamma \\ 0 & \text{else} \end{cases} \quad (13)$$

$$sgorp[3] = sgorp[4] = \begin{cases} 1 & \text{if } |Gra[2] - Gra[6]| \geq \Gamma \\ 0 & \text{else} \end{cases} \quad (14)$$

$$sgorp[5] = sgorp[6] = \begin{cases} 1 & \text{if } |Gra[3] - Gra[7]| \geq \Gamma \\ 0 & \text{else} \end{cases} \quad (15)$$

$$sgorp[7] = sgorp[8] = \begin{cases} 1 & \text{if } |Gra[4] - Gra[8]| \geq \Gamma \\ 0 & \text{else} \end{cases} \quad (16)$$

Here, threshold value Γ is chosen empirically as 0.2. We have used a circular pattern for the set of neighboring pixels because it allows for better texture feature extraction based on the curved lines of the FKP, which is the basis of the highly discriminative coding method proposed in this work. The block diagram of the proposed feature extraction method is depicted in Figure 5.

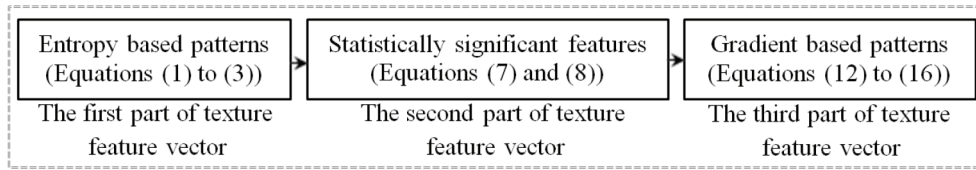


Figure 5. The block diagram of the proposed feature extraction method.

Most of the existing descriptors extract texture structures that are not sufficient for describing the texture information and also not robust against rotation. In local binary patterns, nonuniform patterns are determined with a given value, and the statistical information of the texture patterns does not receive sufficient attention. The rate of cooccurring pixel values for the points positioned at a certain distance and direction from each other is described by a cooccurrence matrix. The closer the pixels are to each other, the greater the concentration on the matrix's main diagonal will be. However, experimental examination showed that this matrix is also not able to accurately identify individuals. Tamura features describe texture characteristics such as roughness, contrast, and orientation. After the empirical investigation, these features and many other texture features were found unable to accurately identify the individuals. The method proposed in this study, however, achieves a higher accuracy by modifying the way the pixels are compared. The high rate of correct identification supports the validity of this claim.

3.4. Selection of superior features using genetic algorithm

This section describes the process of finding the most effective set of texture features by the use of the genetic algorithm. The genetic algorithm is a metaheuristic method for solving optimization problems [30]. This method involves incremental improvement of a population of chromosomes, where each chromosome represents a potential solution. Each chromosome consists of multiple genes; their number and the manner in which they are represented depend on the number of parameters defined for the optimization problem. This algorithm starts with creating a population of solutions and progresses with altering some members of this population to create a new generation. In each generation, solutions with the best fitness function value have a higher chance of being selected for the next generation, and this process of evolution continues until the termination condition is met. Here, the goal is to use the genetic algorithm to find an optimal subset of the solution space. Before doing so, it is necessary to define a suitable structure, including a suitable format for the representation of solutions as chromosomes, an appropriate fitness function, and proper operators for crossover, mutation, and selection. Here, each gene represents a texture feature, which is selected if gene κ has a value of 1, and otherwise not selected. One of the key requirements for using the genetic algorithm is to select a good fitness function. Here, this choice must ensure that the features inside a fit chromosome are able to improve the accuracy of classification. Therefore, we consider the classification accuracy as the measure of fitness and define the fitness function as the ratio of the number of correctly classified samples to the total number of samples.

The process of selecting fit chromosomes is based on the value of the fitness function. The higher the fitness function value of a chromosome, the higher the chance of that chromosome to be selected. The crossover and mutation operators are applied to the selected chromosome to produce the next generation. This is done with the help of the roulette wheel selection operator. The crossover operator is used to ensure a systematic change in chromosomes from one generation to the next. This operator takes two chromosomes and generates two new chromosomes by swapping one or more parts of them with the other. Here, the single-point variant of the crossover operator is used. In this operator, each chromosome is split into two parts from a single randomly

selected point and one of these parts is swapped with the corresponding part in the other chromosome. The uniform mutation operator is used to ensure a small but constant chance of random changes in the population. This operator randomly flips a gene from zero to one or vice versa. Overall, in the genetic algorithm used for feature selection, a population of chromosomes is created randomly. Then the roulette wheel [31] and genetic operators are used to select and modify population members and create a new generation of offspring. After evaluating these offspring, they are added to the pool of the existing population to undergo the selection process. A number of chromosomes with the best fitness values are directly transferred to the next generation. The rest of the generation is formed by the use of the roulette wheel operator. This process continues until the termination condition is met.

3.5. Identity recognition

The pseudocode of the proposed FKP-based identity recognition algorithm is shown in Figure 6. In this system, the received hand images undergo a preprocessing phase, which involves recognizing the hand area by skin color and separating the FKP areas. After extracting distinctive texture features and forming feature vectors, a set of significant features is selected by the genetic algorithm. The obtained FKP pattern is then compared with the dataset. In this step, a feedback scheme is used to refine the search results. In each iteration, this scheme determines the related and unrelated images and updates the system to provide another set of options in the next iteration. This process continues until the target image appears among the retrieved images. The method used here for this purpose is SVM. This linear SVM is trained by the selection of relevant and irrelevant images over multiple iterations. In this training, the related images are tagged with +1 and unrelated images are labeled with -1.

```

for each individual (Hand_image) do
  I_FKP:=Preprocess(Hand_image);
  features:=feature_extraction(I_FKP);
  features_select:=GA(features);
end for
result_SVM := SVM_classification(features_select);
calculate(recognition_rate);
Evaluation(results);

```

Figure 6. The pseudocode of the proposed FKP-based identity recognition system. After training, decision values for the model images are obtained by Equation 17.

$$D(x) = W^T x + bi \quad (17)$$

Here, W is the vector of the separating hyperplane and bi is the bias value. Finally, the similarity criterion is updated by adding the decision value to its value in the previous iteration.

$$S_{t+1}(x) = S_t(x) + D(x) \quad (18)$$

After this updating step, new images are retrieved based on the new value of the similarity criterion. Next, the proposed biometric identification system is evaluated in terms of different criteria.

4. Experimental results

All experiments were carried out on a system with Core i5, 2.5 GHz CPU, and 4 GB memory. Training and testing were performed on the images of the Poly-U FKP and FKP datasets.

The Poly-U FKP dataset contains images taken from 165 people, including 125 men and 40 women, of which 143 are 20–30 years old and the rest are 30–50 years of age. These samples were compiled in two separate parts, each containing 6 images for left and right middle and index fingers. Created by the Hong Kong Polytechnic University,¹ this dataset contains 7920 images from 660 different fingers. The FKP database contains the images taken from the hands of 109 people, 74 males and 35 females, with the age range of 16–69 years. For each person, 5 images from the right hand and 5 images from the left hand have been taken. The authors have compiled this dataset as an alternative set of publicly available hand images for research purposes. The resolution of the FKP area in the images of this dataset is 75×75 pixels. For the purpose of this evaluation, we needed a set of data for training and another for testing. For the training phase, we used 4905 training samples with different hand positions. The genetic algorithm was used to find the most effective features among those extracted. The GA-based feature selection was repeated several times with different parameters. The most suitable settings for this dataset were found to be as follows: initial population = 100, number of generations = 120, mutation type: single-point, mutation rate = 0.05, crossover type: uniform, number of directly transferred (fittest) chromosomes = 35.

In general, biometric systems are judged according to their false acceptance rate (FAR) and false rejection rate (FRR) [21]. Performance of a biometric system can also be evaluated by receiver operating characteristic (ROC) curves. This diagram can be obtained by plotting FRR against FAR for all thresholds. This evaluation can also be performed by the use of the genuine acceptance rate (GAR) as a substitute for FRR. Another performance evaluation method for biometric identification systems is the cumulative match characteristic (CMC) diagram [32]. For this diagram, all samples in the test dataset should also be presented in the training dataset. In this study, the ratio of the number of correctly recognized images to the total number of images is also used as a measure for evaluation. Figures 7a and 7b show, respectively, the ROC and CMC curves of the proposed method for the FKP dataset. Both of these diagrams confirm the effectiveness of the proposed solution. For this dataset, the method has been able to correctly identify about 98% of samples. The high rate of true acceptance in these curves demonstrates the high identification accuracy of the proposed biometric system. In the following, the proposed biometric system is compared with other methods. For this comparison, a number of existing methods were implemented on the FKP dataset. It should be noted that all implementations had identical conditions in terms of input images and the number of images in the training and test sets. First, 4905 images were coded for training with feature extraction, entropy-based pattern histogram, statistical features, and gradient-based patterns. Then performance evaluation was performed using 545 test images. A feedback scheme was also used to improve system performance. The comparison between the results of the tested methods showed that the proposed method has a higher recognition rate for the FKP dataset than others. The results have been implemented on the FKP dataset. In fact, we compared the performance of twelve methods on the FKP dataset. The proposed scheme achieved superior performance. We conclude that the proposed descriptor is very useful. Also, it has the high performance as compared with others (Table 1).

These results illustrate the high performance of the proposed method as compared to other recent methods in the FKP dataset. The implementation of the proposed solution demonstrates the advantages of this system over other biometric systems. It should be noted that the proposed method was able to achieve this level of improvement in accuracy through an easily implemented solution. Note that Table 1 also compares the proposed method with a deep learning approach (DeepTEN)[24]. The DeepTEN result is from another dataset called the

¹PolyU COMP (1974). The PolyU Finger Knuckle Dataset [online]. Website <http://www.Comp.polyu.edu.hk/biometrics> [accessed 23 August 2002].

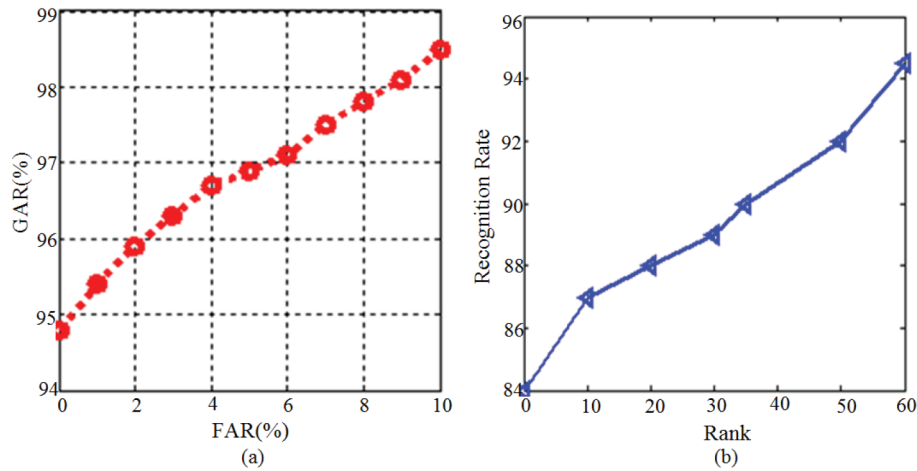


Figure 7. The ROC and CMC curves of the proposed biometric identification system on the FKP dataset.

Table 1. The recognition rates obtained by the proposed method and other methods.

Method	The recognition rate (%)
Local binary patterns [25]	74.32
Median binary patterns [33]	76.46
Improved local binary patterns [34]	86.12
Local ternary patterns [34]	80.81
Robust local binary patterns [34]	71.54
Fuzzy local binary patterns [35]	51.66
Histogram of oriented gradient (HOG) [36]	58.54
Scale-invariant feature transform (SIFT) [37]	39.23
Wavelet transform [38]	74.53
Gabor wavelet [20]	55.47
Local quadruple pattern (LQPAT) [39]	89.88
Local graph structure (LGS) [40]	87.43
Deep texture encoding network (DeepTEN) [24]	80.2
Proposed method on Poly-U FKP dataset	94.91
Proposed method on FKP dataset without gradient based patterns	92.9
Proposed method on FKP dataset	98.5

flickr material dataset. The proposed biometric system exhibits a higher recognition rate than the DeepTEN approach. In addition, according to this table, we observe that the recognition rate with the proposed approach without gradient-based patterns has been decreased from 98.5% to 92.9%. In fact, the third part of the texture feature vector is a particularly important feature with a key role in our application. The proposed descriptor was also able to reach higher recognition accuracy than the other tested methods. On average, this method is 8.62% more accurate than the most accurate algorithm proposed to date (98.5% vs. 89.88%). Overall, it can be claimed that the proposed method has clear superiority over other descriptors in terms of identity recognition. Table 2 shows the time needed to run the different stages of the algorithm for an image. With this

relatively short time of image processing, the proposed biometric system can be used for security and real-time applications.

Table 2. The execution time of different stages of the proposed biometric identification algorithm.

Stages	Time (ms)
Image loading	67
Image preprocessing and FKP extraction	402
Feature extraction	580
Selection of superior features	383
Matching	79

Also, to demonstrate the superiority of the proposed method over other texture descriptors (i.e. 1) local binary pattern [25], 2) median binary pattern [33], 3) improved local binary pattern [34], 4) local ternary pattern [34], 5) robust local binary pattern [34], 6) fuzzy local binary pattern [35], 7) histogram of oriented gradient [36], 8) scale-invariant feature transform [37], 9) wavelet transform [38], 10) Gabor wavelet [20], 11) LQPAT [39], and 12) LGS [40]), in terms of the time complexity, Figure 8 shows the time length of the feature extraction phase in the implemented methods. As illustrated in this figure, the tenth method has the longest feature extraction phase among the tested methods and the proposed method has a shorter feature extraction phase than most other methods.

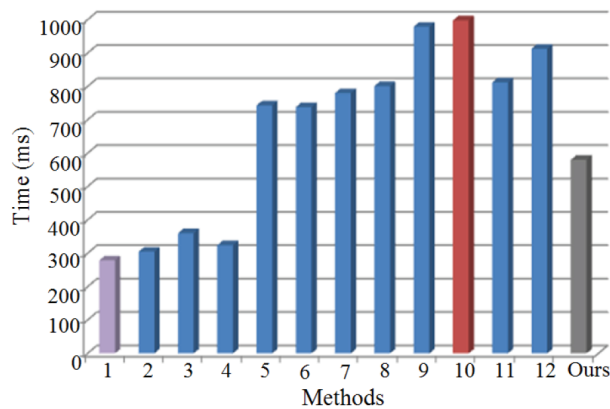


Figure 8. Time taken for feature extraction in milliseconds for FKP image.

5. Conclusion and future works

This paper presented a new method of identity recognition based on FKP features. The proposed method involves creating a dataset of hand images using mapping in the CMYK color space to detect skin regions, using a novel solution to separate the area of interest from the images and extracting features from these areas. Feature extraction was performed on two datasets called Poly-U FKP and FKP by combining the entropy-based histogram of texture patterns at different levels with a set of statistical texture features and gradient-based histogram patterns. The proposed solution is simple yet effective, and as the results suggest, it achieved 94.91% and 98.5% recognition rates in two very large image datasets. This method is able to reach a higher level of performance than the best method currently present in the literature.

In future studies, researchers are recommended to work on biometric systems based on other hand features, including palm lines. Also, the use of graphic processing units and parallel processing for the extraction and computation of visual features can significantly improve the computational speed and therefore the applicability of the solutions.

References

- [1] Swati MR, Ravishankar M. Finger knuckle print recognition based on Gabor feature and KPCA+LDA. In: International Conference on Emerging Trends in Communication, Control, Signal Processing and Computing Applications; Bangalore, India; 2014. pp. 1-5.
- [2] Galbally J, Marcel S, Fierrez J. Image quality assessment for fake biometric detection: application to iris, fingerprint and face recognition. *IEEE Transactions on Image Processing* 2014; 23: 710-724.
- [3] Seetharaman K, Ragupathy R. Iris recognition for personal identification system. *Procedia Engineering* 2016; 38: 1531-1546.
- [4] Grabowski K, Napieralski A. Hardware architecture optimized for iris recognition. *IEEE Transactions on Circuits and Systems for Video Technology* 2011; 9: 1293-1303.
- [5] Dey S, Samanta D. Iris data indexing method using Gabor energy features. *IEEE Transactions on Information Forensics and Security* 2012; 7: 1192-1203.
- [6] Abramoff MD, Garvin MK, Sonka M. Retinal imaging and image analysis. *IEEE Reviews in Biomed Engineering* 2010; 3: 169-208.
- [7] Kose C, Bas CI. A personal identification system using retinal vasculature in retinal fundus image. *Expert Systems with Applications* 2011; 38: 13670-13681.
- [8] Radha R, Lakshman B. Identification of retinal image features using bitplane separation and mathematical morphology. In: World Congress on Computing and Communication Technologies; Trichirappalli, India; 2014. pp. 120-123.
- [9] Bustard JD, Nixon MS. Toward unconstrained ear recognition from two dimensional images. *IEEE Transactions on System, Man, and Cybernetics* 2010; 40: 486-494.
- [10] Kalluri HK. Palm print identification and verification with minimal number of features. *Biometrics* 2018; 10: 16-28.
- [11] Parivazhagan A, Therese A. Face detection cum recognition system using novel techniques for human authentication. *Biometrics* 2018; 10: 315-333.
- [12] Gao G, Yang J, Qian J, Zhang L. Integration of multiple orientation and texture information for finger-knuckle-print verification. *Neurocomputing* 2014; 135: 180-191.
- [13] Zhang L, Zhang D, Guo Z. Phase congruency induced local features for finger-knuckle-print recognition. *Pattern Recognition* 2012; 45: 2522-2531.
- [14] Woodard DL, Flynn PJ. Finger surface as a biometric identifier. *Computer Vision and Image Understanding* 2005; 100: 357-384.
- [15] Ferrer MA, Travieso CM, Alonso JB. Using hand knuckle texture for biometric identification. In: 39th Annual International Carnahan Conference on Security Technology; Las Palmas, Spain; 2006. pp. 1-5.
- [16] Ravikanth C, Kumar A. Biometric authentication using finger back surface. In: IEEE Conference on Computer Vision and Pattern Recognition; Minneapolis, MN, USA; 2007. pp. 1-6.
- [17] Zhao R, Li K, Liu M, Sun X. A novel approach of personal identification based on single knuckle print image. In: Asia-Pacific Conference on Information Processing; Shenzhan, China; 2009. pp. 218-221.
- [18] Shariatmadar ZS, Faez K. A novel approach for finger knuckle print recognition based on Gabor feature fusion. In: 4th International Congress on Image and Signal Processing; Shanghai, China; 2011. pp. 1480-1484.

- [19] Morales A, Travieso CM, Ferrer MA, Alonso JB. Improved finger knuckle print authentication based on orientation enhancement. *Electronic Letters* 2011; 47: 380-381.
- [20] Nigam A, Gupta P. Designing an accurate hand biometric based authentication system fusing finger knuckle print and palmprint. *Neurocomputing* 2015; 151: 1120-1132.
- [21] Ozkaya N, Kurat N. Discriminative common vector based finger knuckle recognition. *Visual Communication and Image Representation* 2014; 25: 1647-1675.
- [22] Grover J, Hanmandlu M. Hybrid fusion of score level and adaptive fuzzy decision level fusions for the finger-knuckle-print based authentication. *Applied Soft Computing* 2015; 31: 1-13.
- [23] Qayyum A, Muhammad SM, Awais M, Majid M. Medical image retrieval using deep convolutional neural network. *Neurocomputing* 2017; 266: 8-20.
- [24] Zhang H, Xue J, Dana K. DeepTEN: texture encoding network. *Computer Vision and Pattern Recognition* 2017; 1: 14-26.
- [25] Pan Z, Li Z, Fan H, Wu X. Feature based local binary pattern for rotation invariant texture classification. *Expert Systems with Applications* 2017; 88: 238-248.
- [26] Silva L, Duque J, Felipe J, Murta L. Two dimensional multiscale entropy analysis: Application to image texture evaluation. *Signal Processing* 2018; 147: 224-232.
- [27] Fathi A, Nagh-Nilchi A. General rotation-invariant local binary patterns operator with application to blood vessel detection in retinal images. *Pattern Analysis and Application* 2014; 17: 69-81.
- [28] Antic A, Popovic B, Krstanovic L, Obradovic R, Milosevic M. Novel texture based descriptors for tool wear condition monitoring. *Mechanical Systems and Signal Processing* 2018; 98: 1-15.
- [29] Sawicki D, Miziolek W. Human colour skin detection in CMYK colour space. *IET Image Processing* 2015; 9: 751-757.
- [30] Zhi H, Liu S. Face recognition based on genetic algorithm. *Visual Communication and Image Representation* 2019; 58: 495-502.
- [31] Back T, Fogel DB, Michalewicz Z. *Handbook of Evolutionary Computation*. Bristol, UK: Institute of Physics, 1997. pp. 1-6.
- [32] De P, Ghoshal D. Recognition of non-circular iris pattern of the goat by structural, statistical and Fourier descriptors. In: *12th International Multi-Conference on Information Processing*; Bangalore, India; 2016. pp. 845-849.
- [33] Harfiane A, Palaniappan K, Seetharaman G. Joint adaptive median binary patterns for texture classification. *Pattern Recognition* 2015; 48: 2609-2620.
- [34] Kylberg G, Sintorn I. Evaluation of noise robustness for local binary pattern descriptors in texture classification. *Image and Video Processing* 2013; 17: 1-20.
- [35] El-Alfy ES, Binsaadoon AG. Silhouette based gender recognition in smart environments using fuzzy local binary patterns and support vector machines. In: *8th International Conference on Ambient Systems, Networks and Technologies*; Madeira, Portugal; 2017. pp. 164-171.
- [36] Jung HG. Analysis of reduced-set construction using image reconstruction from a HOG feature vector. *IET Computing Vision* 2017; 11: 725-732.
- [37] Joo HB, Jeon JW. Feature-point extraction based on an improved SIFT algorithm. In: *17th International Conference on Control, Automation and Systems*; Jeju, South Korea; 2017. pp. 1-5.
- [38] Busch A, Boles WW. Texture classification using multiple wavelet analysis. In: *Digital Image Computing Techniques and Applications*; Melbourne, Australia; 2002. pp. 1-5.
- [39] Chakraborty S, Singh SK, Chakraborty P. Local quadruple pattern: a local descriptor for facial image recognition and retrieval. *Computer and Electrical Engineering* 2017; 62: 92-104.
- [40] Abdullah MFA, Sayeed MS, Muthu KS, Bashier HK, Azman A et al. Face recognition with Symmetric local graph structure (SLGS). *Expert Systems with Applications* 2014; 41: 6131-6137.